Journal of the Optical Society of America B
OPTICAL PHYSICS

Unveiling of control on the polarization of supercontinuum spectra based on ultrafast birefringence induced by filamentation

Ping-Ping Li,[1] Meng-Qiang Cai,[1] Jia-Qi Lü,[1] Dan Wang,[1] Gui-Geng Liu,[1] Chenghou Tu,[1] Yongnan Li,[1,4] and Hui-Tian Wang[2,3,*]

[1]School of Physics and MOE Key Laboratory of Weak Light Nonlinear Photonics, Nankai University, Tianjin 300071, China
[2]National Laboratory of Solid State Microstructures and School of Physics, Nanjing University, Nanjing 210093, China
[3]Collaborative Innovation Center of Advanced Microstructures, Nanjing University, Nanjing 210093, China
[4]e-mail: liyongnan@nankai.edu.cn
*Corresponding author: htwang@nju.edu.cn

Received 17 July 2018; revised 1 October 2018; accepted 2 October 2018; posted 3 October 2018 (Doc. ID 340025); published 29 October 2018

An intensity pump femtosecond (fs) pulse incident into a transparent medium will produce filamentation and accompany supercontinuum (SC) spectrum generation. The polarization of the SC spectrum is always parallel to that of the pump pulse. How to control the polarization of the SC spectrum is a very interesting and crucial issue due to its great potential applications in remote sensing and time-resolved spectroscopy. Here we present a method to control the polarization of the SC spectrum generated in an optical isotropic medium, based on the nonlinear interaction between the two pump pulses with different linear polarizations. During the fs pulse filamentation, the optical Kerr effect induces ultrafast birefringence in the optical isotropic medium, which leads to different refractive indices in the two orthogonal directions parallel and perpendicular to the incident polarization, and hence, the resulting relative phase difference changes the polarizations of the pump pulses. The polarization states of both the pump pulses and the SC spectra can be achieved by changing the angle between the polarization directions of the two pulses. We unveil the mechanism of the polarization changes of the pump pulses and the SC spectra.

https://doi.org/10.1364/JOSAB.35.002916

1. INTRODUCTION

Femtosecond (fs) filamentation, which was first reported by Braun *et al.* [1], occurs when the pulse energy is beyond a critical value; the self-focusing effect produced by the optical Kerr effect will be balanced by the self-diffraction effect and the self-defocussing effect of the plasma. Many effects are accompanied by fs laser filamentation, such as supercontinuum spectrum generation [2–6], terahertz radiation [7–10], and high-order harmonics [11]. A subsidiary effect or phenomenon of filamentation, supercontinuum (SC) generation, has aroused the interest of researchers; it was first discovered by Alfano and Shapiro in 1970 [12] when the intense ultrashort laser pulses were focused into a transparent medium. Owing to its advantages of high spatial coherence, good polarization properties, and spectral brightness, SC generation has found many applications in pulse compression [13,14], remote sensing [15,16], time-resolved spectroscopy [17], fluorescence biomedical imaging [18], material characterization [19,20], and dense wavelength division multiplexing (DWDM) [21–23]. Up to now, many studies have focused on how to regulate the properties of the SC generation, for example, generation of an ultrabroad extreme ultraviolet SC spectrum in a two-color laser field [24] and control of SC generation with polarization of the input laser [25]. However, regulation of the polarization of SC spectra seldom involves the polarization orientations of two pump pulses. In addition, the white light continuum is commonly believed to be polarized in the direction of the input pump pulses for an isotropic medium [12]. Béjot *et al.* [26] demonstrated the substantial birefringence induced by the laser-generated self-guided filaments in gases and realized an ultrafast unprecedented switch under an angle of 45° between the filament and the probe polarizations.

In this paper, we present a method to control the polarization of the SC generation accompanied by fs filamentation, based on the nonlinear interaction between two linearly polarized pulses incident into K9 glass. Because of the ultrafast birefringence produced in the collapsing region of the fs pulses, the ellipticities of the polarization states of both the pump pulses and the SC spectra produced by them can be controlled by the angle θ between polarization directions of two linearly

polarized pulses. One is found in which the changes of the polarization states, the ellipticities of the pump pulses, and the SC spectra produced by them reach their maxima at $\theta = 45°$ and 135°. In contrast, there are no changes at $\theta = 0°$, 90°, and 180°. The experimental results are in good agreement with the theoretical analysis. The scheme we proposed is not limited by the broad band of the polarizer and can accurately change the polarization state of one of the filaments in the stable filamentation. It is then possible to control the SC spectrum produced by the filaments, so our scheme should have potential applications.

2. EXPERIMENT

The experimental setup is shown in Fig. 1. The light source we used is a fs Ti-sapphire regenerative amplifier (Coherent Inc.) operating at a central wavelength of 800 nm, a pulse duration of 35 fs, and a repetition rate of 1 kHz, which delivers a fundamental Gaussian mode. The total energy of the input fs pulse is controlled by a combination of an achromatic half-wave plate (HWP1) and a polarization beam splitter (PBS1). After the second PBS2, the input fs pulse is divided into two paths (Path-1 and Path-2), and then they meet in the optical isotropic K9 glass through two reflectors (the modified Mach–Zehnder interferometer). HWP2 in the front of PBS2 is used to adjust the relative energy fraction of the two pump pulses in the two paths. HWP3 and HWP4 inserted in the two paths are used to change the polarization directions of the two pump pulses incident in the K9 glass with a dimension of $15 \times 15 \times 3$ mm^3. Lens L1 with a long focal length of $f_{L1} = 1000$ mm makes the focal points of two pump pulses be in the front of the geometric intersection. The focusing effect is mainly completed by lens L2 with a short focal length of $f_{L2} = 350$ mm. Behind the K9 glass, a pair of lenses (L3 and L4) are used to collect the conical emission SC light into the fiber-based spectrometer (USB4000VIS-NIR). We must emphasize that an infrared cut-off filter near 750 nm is always inserted in the front of the spectrometer to ensure the detected SC spectra within a range of 450–750 nm. Delay lines in the two paths are used to change the relative time retardation between the two pump pulses in the two paths. In Fig. 1, we label the two pump pulses in Path-1 and the Path-2 as Pulse-1 and Pulse-2, respectively.

First, we explore the dependence of the SC spectrum in the total intensity [Fig. 2(a)], the horizontal component [Fig. 2(b)], and the vertical component [Fig. 2(c)] of Pulse-1 on the polarization direction of Pulse-2. Pulse-1 and Pulse-2 are both linearly polarized. We should point out that the polarization of Pulse-1 is always in the horizontal direction, which is defined as the x direction, and correspondingly, the vertical direction is defined as the y direction. In addition, we define the angle between the polarization directions of Pulse-1 and Pulse-2 as θ. The input average power of the two pump pulses are $P_1 = 23.312$ mW and $P_2 = 24.176$ mW, respectively. The polarization direction of Pulse-2 can change from $\theta = 0°$ to 180°. The integration time of the spectrometer is 100 ms, meaning that this time window includes 100 pulses, and the average number is 1690 times. In the front of the spectrometer, we insert a neutral attenuator set with a transmissivity of ~0.63‰ for Fig. 2(a) and ~1‰ for Figs. 2(b) and 2(c) to avoid the spectrum being too strong. As shown in Fig. 2(a), the total intensity of the SC spectrum for Pulse-1 exhibits a periodic oscillation with a period of 90° as the polarization direction of Pulse-2 changes, where the maxima are located at $\theta = 0°$, 90°, and 180°, while the minima are located at $\theta = 45°$ and 135°. For the sake of brevity, the SC spectra for Pulse-1 and Pulse-2 are abbreviated as SC-1 and SC-2 spectra, respectively. To investigate the effect of interaction between the two filaments on the polarization properties of the SC spectra, we also measure the x and y components of the SC-1 spectrum under different θ. Experimental results show that both exhibit a periodicity. The x component [Fig. 2(b)] is very similar to the periodic behavior of the total intensity [Fig. 2(a)], whereas the y component [Fig. 2(c)] exhibits an opposite (or complementary) behavior to the total intensity and the x component. This means that the ellipticity of the SC-1 spectrum varies with the angle θ and reaches a maximum when θ is 45°. The intensity of the generated SC spectrum depends on the polarization

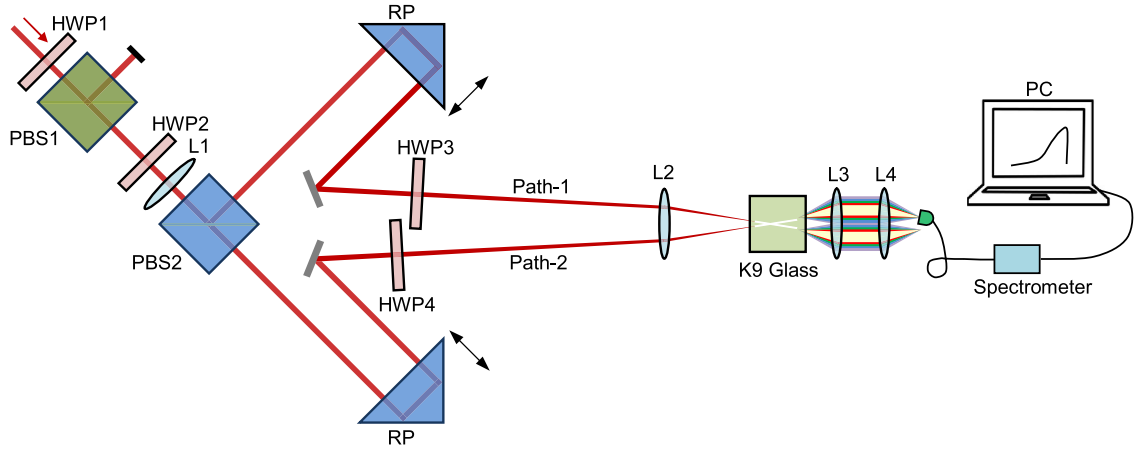

Fig. 1. Experimental setup for controlling the SC spectra based on the interaction between the two pump pulses in a modified MZ interferometer. HWP, half-wave plate; PBS, polarized beam splitter; RP, rectangular prism; L1, L2, L3 and L4, convex lenses. L1 and L2 have focal lengths of $f_{L1} = 1000$ mm and $f_{L2} = 350$ mm, while L3 and L4 have different focal lengths for different measurements. In Fig. 3, $f_{L3} = 60$ mm and $f_{L4} = 50$ mm; in Figs. 4(c) and 6, only L3 is used with $f_{L3} = 60$ mm; in other figures, $f_{L3} = 60$ mm and $f_{L4} = 200$ mm.

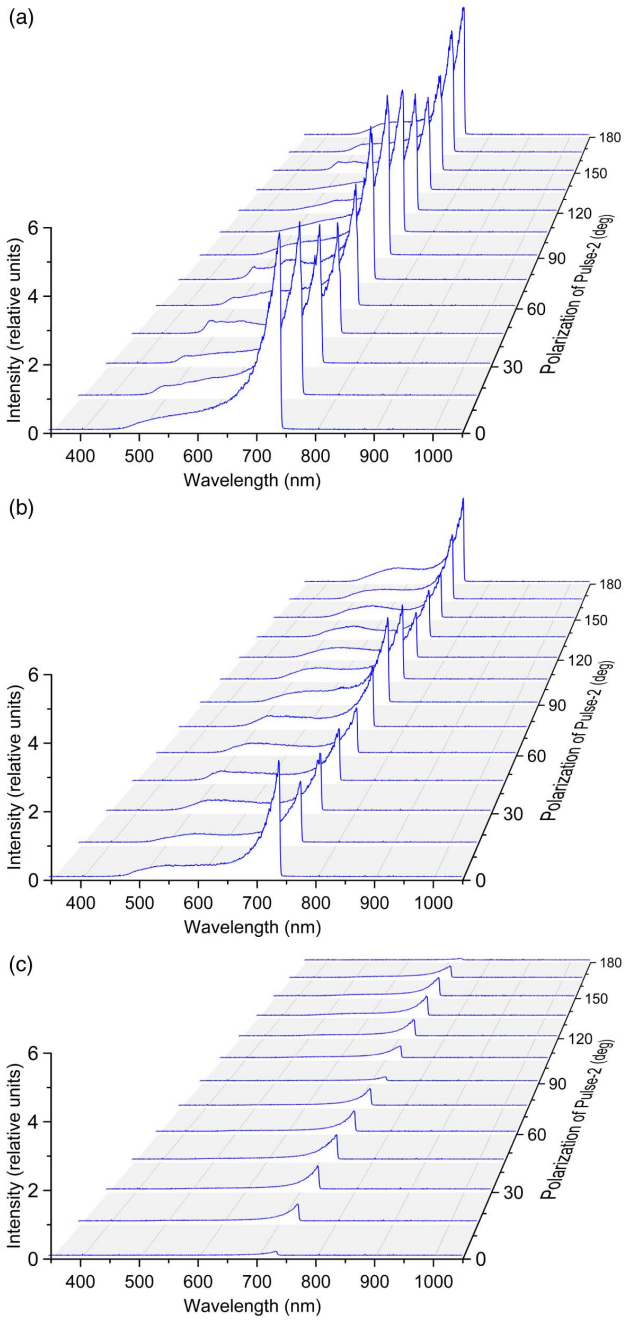

Fig. 2. Dependence of the SC spectrum of Pulse-1 on the polarization direction of Pulse-2. (a) The total intensity, (b) the horizontal component, and (c) the vertical component.

of the incident laser pulses and increases as the polarization changes from a circular polarization to a linear one, regardless of the sample, as in Ref. [25]. This is also the reason why the maxima of the total intensity of the SC spectrum for Pulse-1 are located at $\theta = 0°$, 90°, and 180°, while the minima are located at $\theta = 45°$ and 135°. Therefore, we can continuously control the polarization state of the SC spectrum by interacting with another pulsed beam.

For the purpose of more vividly and comprehensively understanding the polarization property of the SC spectrum, we capture the sectional view of the SC spectrum behind a polarizer, as shown in Fig. 3, when the two pump pulses have the input average power of $P_1 = 14.334$ mW and $P_2 = 14.174$ mW at $\theta = 0°$ and 45°, respectively. We used a neutral attenuator with its transmissivity of 3.2‰. To eliminate the effect of aberration on imaging, we used a $4f$ system including a small phihole to allow only the SC-1 spectrum to pass. We can find from Fig. 3 that when Pulse-2 is absent, the polarization property of the SC-1 spectrum is basically the same as Pulse-1, which is x polarized; whereas, in the presence of Pulse-2 at $\theta = 45°$, the SC-1 spectrum includes the y component, indicating that Pulse-2 has a large influence on the polarization properties of the SC-1 spectrum and vice versa.

3. DISCUSSION

In order to reveal the mechanism of the polarization change of the SC spectrum, we should explore whether the polarization changes of Pulse-1 and Pulse-2 are related to the filamentation. In the experimental results shown in Figs. 4(a) and 4(b), we keep the two pump pulses with the same input power ($P_1 = P_2$) and zero delay. As mentioned above, Pulse-1 is always x polarization, while Pulse-2 is at $\theta = 45°$ linear polarization. We insert a band-pass filter with a central wavelength of 800 nm and a full width at half-maximum (FWHM) of 10 nm behind the K9 glass to ensure that only the pump pulses at 800 nm can enter the power meter. In Fig. 4(a), Pulse-1 and Pulse-2 have the same input power of $P_1 = P_2 = 3.1430$ mW, which is insufficient for the filamentation. In Fig. 4(a), a neutral attenuator with a transmissivity of 32% is inserted in front of the power meter. Clearly, in this case, the interaction between the two pump pulses does not result in any change in the total power (P_{1T} and P_{2T}), the x-component power (P_{1x} and P_{2x}), or the y-component power (P_{1y} and P_{2y}) for the two pulses transmitted from the K9 glass. As a comparison, in Fig. 4(b), Pulse-1 and Pulse-2 have the same input power of $P_1 = P_2 = 9.3586$ mW, which is enough to produce the filamentation even accompanying the SC generation. As shown in Fig. 4(b), the interaction between the two pump pulses gives rise to the increase (decrease) of P_{1T} (P_{2T}), the decrease (increase) of P_{1x} (P_{2x}), and the increase (decrease) of P_{1y} (P_{2y}). This implies that the changes of the polarization states of the two pulses are closely related to the filamentation. In addition, we also explore the influence of the polarization direction of Pulse-2 on the y-component power (P_{1y}), as shown in Fig. 4(c). One should point out that in Fig. 4(c), the input power of Pulse-1 is not enough for filamentation. The red and blue curves are the sine fitting of the experimental data. We can see that the change of the y-component power (P_{1y}) is in agreement with the change of the y component of the SC-1 spectrum for Pulse-1 [Fig. 2(c)]. When the polarization direction of Pulse-2 is at $\theta = 0°$, 90°, and 180°, in particular, the power of Pulse-1 has no change; correspondingly, the power of Pulse-2 should have also no change, meaning that there is no interaction between the two pulses. In contrast, P_{1y} reaches its maxima when the polarization direction of Pulse-2 is at $\theta = 45°$ and 135°, and P_{1y} becomes higher as the power of the input pulses increases. The results reveal again that when the angle between

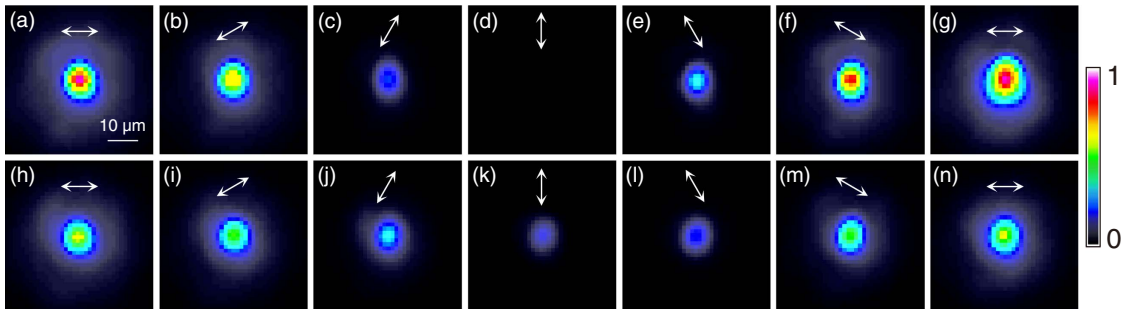

Fig. 3. Polarization properties of SC-1 spectrum captured by the CCD camera. White arrows represent the transmission direction of the polarizer in the front of the CCD, and the color is only on behalf of the spectral intensity. (a)–(g) represent the intensity of the sectional view of the SC-1 spectrum when Pulse-2 is absent, and (h)–(n) represent when Pulse-2 is present.

the polarization directions of the two pump pulses are at $\theta = 45°$ or 135°, both have the strongest interaction.

In order to understand more comprehensively the change of the polarization state of Pulse-1 during the interaction between the two filaments, we measure the Stokes parameter S_3 (characted by Stokes parameter S_3 in Poincaré presentation for a polarization state) of Pulse-1 and Pulse-2, under different input powers, as shown in Fig. 5. During the measurement, a neutral attenuator with a transmissivity of 25.3% is inserted. In Fig. 5, all the curves are the sine fitting of the experimental data.

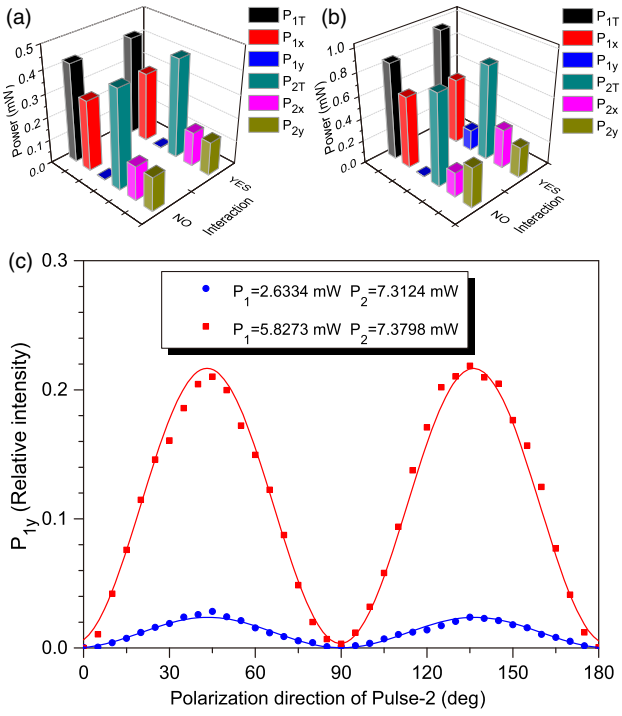

Fig. 4. Power of Pulse-1 and Pulse-2 transmitted from the K9 glass. (a) and (b) show the total power, horizontal (x), and vertical (y) components of Pulse-1 and Pulse-2 when the interaction exists or and when it does not. (a) and (b) correspond to the cases under the input power of $P_1 = P_2 = 3.1430$ mW and $P_1 = P_2 = 9.3586$ mW, respectively. (c) shows the dependence of the power of the y component for Pulse-1 on the polarization direction of Pulse-2 under different input powers for Pulse-1 and Pulse-2.

Clearly, when the initial polarization direction of Pulse-2 is at $\theta = 0°$, 90°, and 180°, the polarization states of Pulse-1 and Pulse-2 have no change to keep the initial linear polarization, i.e., $S_3 \cong 0$. When the initial polarization direction of Pulse-2 is changed from $\theta = 0°$ to 90°, S_3 of Pulse-1 becomes negative, while S_3 of Pulse-2 is positive. That is to say, the polarization state of Pulse-1 (Pulse-2) becomes left-handed (right-handed) elliptic polarization. In contrast, when the initial polarization direction of Pulse-2 is changed from $\theta = 90°$ to 180°, the handedness of the polarization states of Pulse-1 and Pulse-2 are both reversed. $|S_3|$ of Pulse-1 and Pulse-2 reache their maxima at $\theta = 45°$ and 135°, implying that in this case the two pulses have the strongest interaction. The changes of $|S_3|$ for Pulse-1 and Pulse-2 increase as the input power increases. The properties are in agreement with the results shown in Fig. 4.

When intense ultra-short pulses are incident into the nonlinear medium, the filaments will be generated based on the optical Kerr effect, and the light-induced birefringence—the so-called ultrafast birefringence—will also be produced in the region of filamentation. The induced third-order nonlinear polarizations can be different in the x and y orthogonal directions. The third-order nonlinear polarizations in an optical isotropic nonlinear medium can be written as [27]

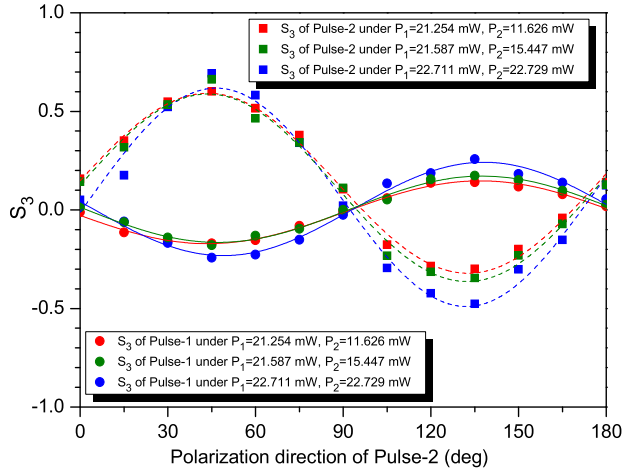

Fig. 5. Dependence of S_3 for both Pulse-1 and Pulse-2 on the polarization direction of Pulse-2 under different incident powers.

$$P_i'^{(3)} = \sum_i [\chi^{(3)}_{1122} E_i' E_j'' E_j''^* + \chi^{(3)}_{1212} E_j' E_i'' E_j''^* + \chi^{(3)}_{1221} E_j' E_j'' E_i''^*], \quad (1)$$

where $i, j = x$ or y. Superscripts, $'$ and $''$ stand for Pulse-1 and Pulse-2, respectively. In order to describe our issue more accurately, the self-phase modulation should be indeed considered. However, for studying the interaction of two beams, the cross-phase modulation is dominant, so self-phase modulation was not written into Eq. (1). In the case when the polarization directions of Pulse-1 and Pulse-2 are at 0° and 45°, respectively, the x and y components of the third-order nonlinear polarization for Pulse-1 are expressed as

$$P_x'^{(3)} = (\chi^{(3)}_{1122} + \chi^{(3)}_{1212} + \chi^{(3)}_{1221}) E_x' E_x'' E_x''^* + \chi^{(3)}_{1122} E_x' E_y'' E_y''^*,$$
$$P_y'^{(3)} = \chi^{(3)}_{1212} E_x' E_y'' E_x''^* + \chi^{(3)}_{1221} E_x' E_x'' E_y''^*. \quad (2)$$

For Pulse-2, the x and y components of the third-order nonlinear polarization are expressed as

$$P_x''^{(3)} = (\chi^{(3)}_{1122} + \chi^{(3)}_{1212} + \chi^{(3)}_{1221}) E_x'' E_x' E_x'^*,$$
$$P_y''^{(3)} = \chi^{(3)}_{1122} E_y'' E_x' E_x'^*. \quad (3)$$

Thus, for Pulse-2, the light-induced anisotropy in susceptibility should be $\Delta\chi = (\chi^{(3)}_{1212} + \chi^{(3)}_{1221})|E_x'|^2$, and then the induced birefringence should be $\Delta n \propto \Delta\chi = (\chi^{(3)}_{1212} + \chi^{(3)}_{1221})|E_x'|^2$. As a result, the x and y components for Pulse-2 introduce a relative phase difference $\Delta\phi'' = \Delta nkl$ (where k and l are the wavevector of light and the interaction length of two pulses in the nonlinear medium), which will change the polarization state of the pump pulses themselves and the induced SC spectra. Based on Eqs. (2) and (3), we easily obtain the Stokes parameter S_3'' for Pulse-2 and the Stokes parameter S_3' and the vertical component E_y' for Pulse-1, as follows:

$$S_3' = -|E'|^2 \sin 2\theta \sin \Delta\phi', \quad (4a)$$

$$S_3'' = |E''|^2 \sin 2\theta \sin \Delta\phi'', \quad (4b)$$

$$E_y' = \frac{1}{2} E_x' \sin 2\theta [1 - \exp(i\Delta\phi')]. \quad (4c)$$

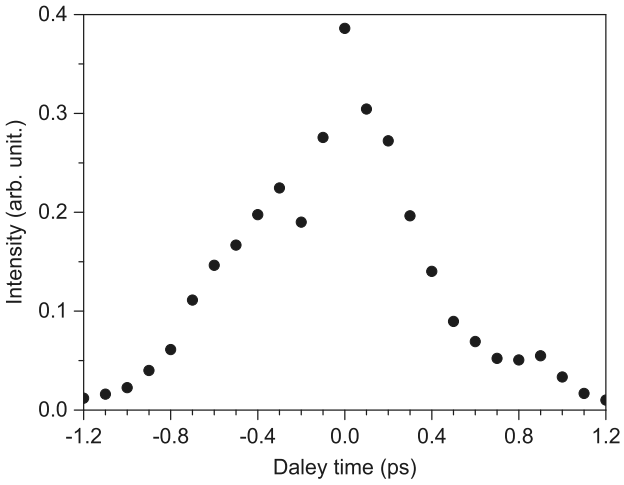

Fig. 6. Dependence of the vertical component of Pulse-1 on the delay time between the two pump pulses.

The above expressions can provide good understanding of Figs. 4(c) and 5. In particular, S_3 for both Pulse-1 and Pulse-2 has opposite signs. As shown in Eq. (4), when $\theta = 0°$, 90°, and 180°, we have $S_3' = S_3'' = 0$ and $E_y' = 0$, implying that the polarization states of Pulse-1 and Pulse-2 have no change. When $\theta = 45°$ and 135°, $|S_3'|$, $|S_3''|$, and $|E_y'|$ have their maxima; that is to say, the polarization states of Pulse-1 and Pulse-2 have the largest change.

We also measure the dependence of the vertical component of Pulse-1 on the delay time between the two pump pulses, as

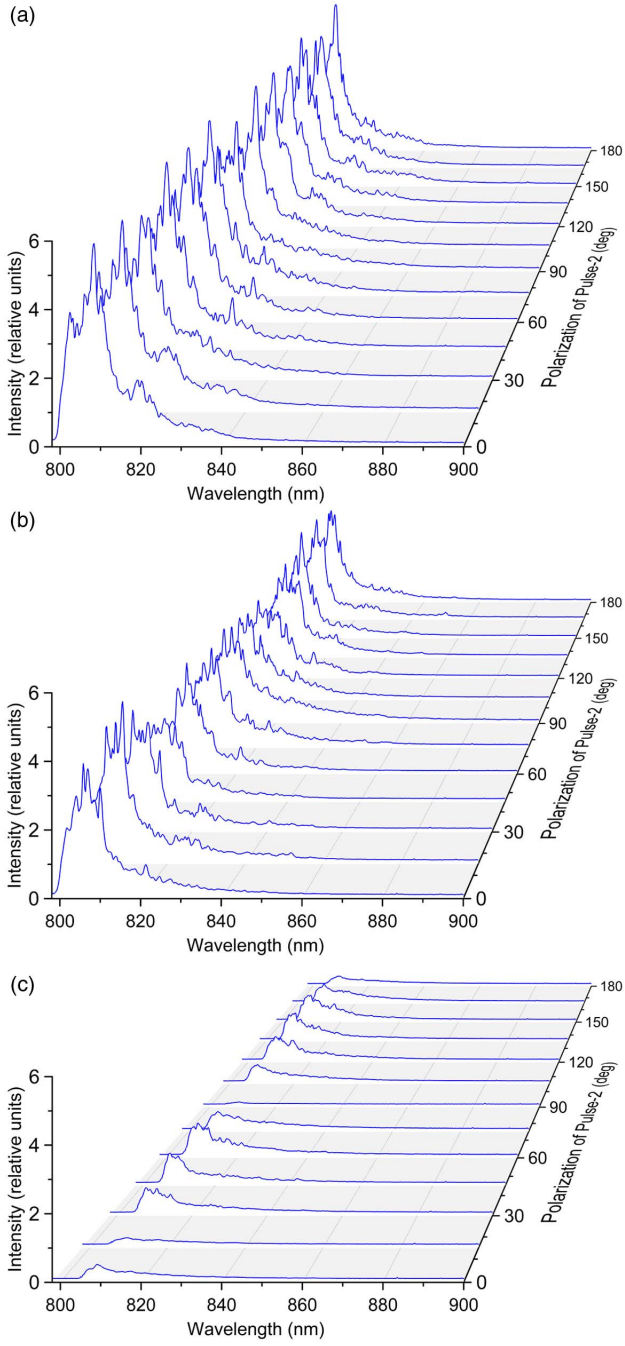

Fig. 7. Dependence of the SC spectrum longer than 800 nm of Pulse-1 on the polarization direction of Pulse-2. (a) The total intensity, (b) the x component, and (c) the y component.

shown in Fig. 6. Clearly, when the delay is ~1.2 ps, the vertical component of Pulse-1 is negligible, implying that the interaction between the two pulses disappears when the delay is beyond 1.2 ps.

Finally, we explore the polarization property of a SC spectrum longer than 800 nm. Similar to Fig. 2, we measure the dependence of the total intensity [Fig. 7(a)], the x component [Fig. 7(b)], and the y component [Fig. 7(c)] of Pulse-1 on the polarization direction of Pulse-2. In our experiments, the two pump pulses have the input average power of $P_1 = 16.781$ mW and $P_2 = 16.694$ mW, the average number of the spectrometer is 1000 times, the SC spectrum shorter than 800 nm is blocked by a cut-off filter, and then the SC spectrum is reduced by a neutral attenuator set with a transmissivity of 0.032‰. As shown in Fig. 7, the total intensity, x component, and y component of the SC-1 spectrum above 800 nm exhibit a periodic oscillation with a period of 90°, although the oscillation is not very clear. For the total intensity [Fig. 7(a)] and the x component [Fig. 7(b)], their maxima are locate at $\theta = 0°$, 90°, and 180°, while the minima are located at $\theta = 45°$ and 135°. In contrast, the y component in [Fig. 7(c)] exhibits an opposite behavior to the former two. This means that the change of polarization state of the SC-1 spectrum above 800 nm is similar to that in the short-wavelength region shown in Fig 2.

4. CONCLUSION

In summary, we have proposed a method to regulate the polarization states of the SC spectra generated in the optical isotropic medium during the filamentation of fs pulses. When two pulses are incident into the isotropic medium, because of the ultrafast birefringence induced by the filaments, the polarization states of the two pulses and the SC spectra depend on the angle between the input polarization directions and their power. In particular, these changes achieve their maxima when the angle is at 45° and 135°, while there is no change when the angle is at 0°, 90°, and 180°, independent of the input power. We reveal that all these phenomena originate from the mechanism of nonlinear coupling between the two filaments produced by the two strong fs pulses. Our research content is essentially different from that of Ref. [26]. One of our main questions is how to change the polarization states of the SC spectra. Moreover, this effect can be achieved not only when the angle is 45 deg, as long as the polarizations of the two pulses are not parallel or orthogonal. We only use this scheme to introduce another pulse (even it is not enough to generate the filament), and then the polarization states can be arbitrarily changed. Our scheme should have great potential applications in remote sensing and time-resolved spectroscopy.

Funding. National Key R&D Program of China (2017YFA0303700, 2017YFA0303800); National Natural Science Foundation of China (NSFC) (11534006, 11674184, 11774183); Natural Science Foundation of Tianjin City (16JCZDJC31300); 111 Project (B07013).

Acknowledgment. This work is supported by the Collaborative Innovation Center of Extreme Optics.

REFERENCES

1. A. Braun, G. Korn, X. Liu, D. Du, J. Squier, and G. Mourou, "Self-channeling of high-peak-power femtosecond laser pulses in air," Opt. Lett. **20**, 73–75 (1995).
2. S. Rostami, M. Chini, K. Lim, J. P. Palastro, M. Durand, J. C. Diels, L. Arissian, M. Baudelet, and M. Richardson, "Dramatic enhancement of supercontinuum generation in elliptically-polarized laser filaments," Sci. Rep. **6**, 20363 (2016).
3. F. Silva, D. R. Austin, A. Thai, M. Baudisch, M. Hemmer, D. Faccio, A. Couairon, and J. Biegert, "Multi-octave supercontinuum generation from mid-infrared filamentation in a bulk crystal," Nat. Commun. **3**, 807 (2012).
4. Y. Zhong, H. Diao, Z. Zeng, Y. Zheng, X. Ge, R. X. Li, and Z. Z. Xu, "CEP-controlled supercontinuum generation during filamentation with mid-infrared laser pulse," Opt. Express **22**, 29170–29178 (2014).
5. J. Galinis, G. Tamošauskas, I. Gražulevičiūtė, E. Keblytė, V. Jukna, and A. Dubietis, "Filamentation and supercontinuum generation in solid-state dielectric media with picosecond laser pulses," Phys. Rev. A **92**, 033857 (2015).
6. L. Zhang, T. Xi, Z. Hao, and J. Lin, "Supercontinuum accumulation along a single femtosecond filament in fused silica," J. Phys. D **49**, 115201 (2016).
7. C. D'Amico, A. Houard, M. Franco, B. Prade, A. Mysyrowicz, A. Couairon, and V. T. Tikhonchuk, "Conical forward THz emission from femtosecond-laser-beam filamentation in air," Phys. Rev. Lett. **98**, 235002 (2007).
8. C. D. Amico, A. Houard, S. Akturk, Y. Liu, J. L. Bloas, M. Franco, B. Prade, A. Couairon, V. T. Tikhonchuk, and A. Mysyrowicz, "Forward THz radiation emission by femtosecond filamentation in gases: theory and experiment," New J. Phys. **10**, 013015 (2008).
9. Y. Liu, A. Houard, B. Prade, S. Akturk, A. Mysyrowicz, and V. T. Tikhonchuk, "Terahertz radiation source in air based on bifilamentation of femtosecond laser pulses," Phys. Rev. Lett. **99**, 135002 (2007).
10. J. Zhao, W. Chu, L. Guo, Z. Wang, J. Yang, W. Liu, Y. Cheng, and Z. Xu, "Terahertz imaging with sub-wavelength resolution by femtosecond laser filament in air," Sci. Rep. **4**, 3880 (2014).
11. R. A. Ganeev and H. Kuroda, "Extremely broadened high-order harmonics generated by the femtosecond pulses propagating through the filaments in air," Appl. Phys. Lett. **95**, 201117 (2009).
12. R. R. Alfano and S. L. Shapiro, "Emission in the region 4000 to 7000 Å via four-photon coupling in glass," Phys. Rev. Lett. **24**, 584–587 (1970).
13. R. L. Fork, C. H. B. Cruz, P. C. Becker, and C. V. Shank, "Compression of optical pulses to six femtoseconds by using cubic phase compensation," Opt. Lett. **12**, 483–485 (1987).
14. E. T. J. Nibbering, O. Dühr, and G. Korn, "Generation of intense tunable 20-fs pulses near 400 nm by use of a gas-filled hollow waveguide," Opt. Lett. **22**, 1335–1337 (1997).
15. P. Rairoux, H. Schillinger, S. Niedermeier, M. Rodriguez, F. Ronneberger, R. Sauerbrey, B. Stein, D. Waite, C. Wedekind, H. Wille, L. Wöste, and C. Ziener, "Remote sensing of the atmosphere using ultrashort laser pulses," Appl. Phys. B **71**, 573–580 (2000).
16. J. Kasparian, R. Sauerbrey, D. Mondelain, S. Niedermeier, J. Yu, J. P. Wolf, Y. B. André, M. Franco, B. Prade, S. Tzortzakis, A. Mysyrowicz, M. Rodriguez, H. Wille, and L. Wöste, "Infrared extension of the supercontinuum generated by femtosecond terawatt laser pulses propagating in the atmosphere," Opt. Lett. **25**, 1397–1399 (2000).
17. J. Swartling, A. Bassi, C. D'Andrea, A. Pifferi, A. Torricelli, and R. Cubeddu, "Dynamic time-resolved diffuse spectroscopy based on supercontinuum light pulses," Appl. Opt. **44**, 4684–4692 (2005).
18. C. Dunsby, P. M. P. Lanigan, J. McGinty, D. S. Elson, J. Requejo-Isidro, I. Munro, N. Galletly, F. McCann, B. Treanor, B. Önfelt, D. M. Davis, M. A. A. Neil, and P. M. W. French, "An electronically tunable ultrafast laser source applied to fluorescence imaging and fluorescence lifetime imaging microscopy," J. Phys. D **37**, 3296–3303 (2004).

19. L. D. Boni, A. A. Andrade, L. Misoguti, C. R. Mendonça, and S. C. Zilio, "Z-scan measurements using femtosecond continuum generation," Opt. Express **12**, 3921–3927 (2004).
20. M. Balu, J. Hales, D. J. Hagan, and E. W. V. Stryland, "White-light continuum Z-scan technique for nonlinear materials characterization," Opt. Express **12**, 3820–3826 (2004).
21. I. Zeylikovich, V. Kartazaev, and R. R. Alfano, "Spectral, temporal, and coherence properties of supercontinuum generation in microstructure fiber," J. Opt. Soc. Am. B **22**, 1453–1460 (2005).
22. Ö. Boyraz and M. N. Islam, "A multiwavelength CW source based on longitudinal mode-carving of supercontinuum generated in fibers and noise performance," J. Lightwave Technol. **20**, 1493–1499 (2002).
23. H. Takara, T. Ohara, T. Yamamoto, H. Masuda, M. Abe, H. Takahashi, and T. Morioka, "Field demonstration of over 1000-channel DWDM transmission with supercontinuum multi-carrier source," Electron. Lett. **41**, 270–271 (2005).
24. Z. Zeng, Y. Cheng, X. Song, R. X. Li, and Z. Z. Xu, "Generation of an extreme ultraviolet supercontinuum in a two-color laser field," Phys. Rev. Lett. **98**, 203901 (2007).
25. A. Srivastava and D. Goswami, "Control of supercontinuum generation with polarization of incident laser pulses," Appl. Phys. B **77**, 325–328 (2003).
26. P. Béjot, Y. Petit, L. Bonacina, J. Kasparian, M. Moret, and J. P. Wolf, "Ultrafast gaseous 'half-wave plate'," Opt. Express **16**, 7564–7570 (2008).
27. Y. R. Shen, *The Principles of Nonlinear Optics* (Wiley-Interscience, 1984), p. 317.